What Tells Geometrical Reciprocity about Mass Constituents of the Universe and the Universe itself?

Hans Hermann Otto

Materials Science and Crystallography, Clausthal University of Technology,
Clausthal-Zellerfeld, Lower Saxony, Germany
E-mail: hhermann.otto@web.de

Abstract

The universe is the result of long-lasting stochastic processes in nature, and life is the most complex result of such combined actions of statistics and probability. All these processes occur in the corset of geometry. In this way, natural numbers and their combinations play a dominant role in understanding the fractal universe and its cyclic behavior. We must consider all underlying exact or almost exact relations and reciprocity relations between fundamental numbers that importantly influence statistics, probability and pairing as well as de-pairing behavior. The folding of *DNA*, for example, is a result of such geometric (besides energetic) considerations. In the parlance of photosynthesis or its newly created artificial pendant such number systems may be considered as number catalysts.

Keywords: *DNA* Genetic Code, *DNA* Resonance Code, Qartic Polymial, Golden Mean, Fifth Power of the Golden Mean, *Fiboacci* Number 13, Fractal, α-Helix, Icosahedron Equation, Number Theory, Quantum Computation, Consciousness, Dark Matter, Dark Energy, Electron Structure Model, Geometric Frustration, Cyclic Universe, Vacuum Energy Field.

1. Introduction

The idea is inspiring and really exiting that highly effective synthetic chlorophyll replacements in living plants could one day be reproduced there and then are able to balance the world's CO_2 content sustainably and beneficially for the climate [1]. Life has been created once with its manifested helical structure due to the action of magnetic minerals such as magnetite. The study of *Deng*, *Yu* and *Blackmond* about symmetry breaking and chiral amplification in prebiotic ligand reactions paw the way to synthesize magnetically induced organic composites of opposite chirality [2].

Not equipped with large laboratory equipment or financial resources in the eve of my life, I have to limit myself to the infinite repeatability in natural processes, expressed by fundamental quantities, reciprocity relations and pure geometry, and to an accompanying philosophical assessment. Even if we advance to ever smaller dimensions, nature will produce similar structures because the corset of geometry and mathematics is always the same. It is not only a philosophical question. We need to ask more often what is not there instead of

asking what is there. Crystal faces grow to a large extent because molecules or energy fields are rejected from it, but instead matter is deposited on the edges of the faces.
Some arguments in this contribution are certainly intuitive. However, intuition is the dark component of accumulated huge knowledge of capable individuals and can deliver heuristic solutions and new didactic insights.

2. Relations between Fundamental Numbers

Fundamental numbers, obviously strong related to each other and to geometric bodies such as the icosahedron, are prerequisites of life and universe. For instance, the well approximated relation between the golden mean φ respectively its powers and the circle constant π is fascinating and has far-reaching consequences for the real world [3]

$$\varphi = 0.6180339887\ldots \approx \frac{1}{2}\left(1 + \sqrt{\frac{6}{5\pi}} - \frac{6}{5\pi}\right) = 0.61803343 \tag{1a}$$

$$\Phi = 1.6180339887\ldots \approx \frac{1}{2}\left(3 + \sqrt{\frac{6}{5\pi}} - \frac{6}{5\pi}\right) = 1.61803343 \tag{1b}$$

$$\varphi^2 = 0.38196601\ldots \approx \frac{1}{2}\left(1 - \sqrt{\frac{6}{5\pi}} + \frac{6}{5\pi}\right) = 0.38196657 \tag{1c}$$

$$\varphi^3 = 0.2360679\ldots \approx \sqrt{\frac{6}{5\pi}} - \frac{6}{5\pi} = 0.23606685 \tag{1d}$$

$$\varphi^5 = 0.09016994\ldots \approx \frac{5}{2}\left(\sqrt{\frac{6}{5\pi}} - \frac{6}{5\pi}\right) - \frac{1}{2} = 0.0901671 \tag{1e}$$

Another relation between φ and π was given some years ago [4].

We can approximate the circle constant using icosahedron mathematics. For the regular icosahedron the dihedral angle between two adjacent triangles is

$$\arccos\left(-\frac{\sqrt{5}}{3}\right) = 138.189251° \tag{2a}$$

$$\sin(138.189251) = 2/3 \tag{2b}$$

$$\pi \approx \frac{\sqrt{\frac{2}{3}}}{\sqrt[3]{2}-1} = 3.141325 \tag{2c}$$

The special *Lorentz* factor $\gamma_1 = \sqrt[3]{2} = 1.25992105\ldots$ (2d)

is explained below in more detail.

In the same way, the representation of the inverse of *Sommerfeld*'s omnipresent structure constant α^{-1} by equations of solely the circle constant respectively the golden mean is intriguing [5] [5a]

$$\alpha^{-1} \approx 4\pi^3 + \pi(\pi + 1) = 137.03630 \tag{3a}$$

$$\alpha^{-1} \approx 5^3(1+\varphi^5) + 2\cdot\varphi^2 = 137.03517 \quad (3b)$$

Also the fractal part of the gyromagnetic factor of the electron can be approximated by solely π-based terms

$$\Delta g_e \approx \frac{1}{4\pi^4+\pi^2(\pi+1)+\frac{2}{\pi}} = 0.00231939\ldots \quad (3c)$$

In addition, the following relation that combines φ and α^{-1} respectively π near number 13 is remarkable

$$\sqrt{2\varphi/\alpha} = 13.01482999\ldots \approx \pi(\pi+1) = 13.011197 \quad (4)$$

All three almost omnipresent numbers φ, π, and α are needed to describe continuous rotation and precession movement of matter and are in addition related to the icosahedron as important chiral structural building unit, for instance observed in life as virus structures. Recently, programmable icosahedral *DNA* shell structures could be constructed for virus trapping as potential application [6]. Because nature repeated structures again and again, one day icosahedral networks could be found also in sub-particle structures.

Interestingly, our icosahedral *Moebius* ball electron model [7] delivers a connection between the icosahedron, the golden mean and the inverse of *Sommerfeld*'s structure constant $\alpha^{-1} = 137.035999177(21)$ [8]

$$\frac{4}{5}171 + \varphi^3 = \frac{3}{5}228 + \varphi^3 = 136.8 + 0.2360 = 137.0360 \quad (5a)$$

$$\frac{171-\Phi}{2\varphi} = 137.0329 \quad (5b)$$

$$\frac{\left(13+\frac{1}{13}\right)^2-\Phi}{2\varphi} = 137.0376 \quad (5c)$$

where numbers 171 respectively 228 are coefficients of the icosahedron equation [9].

If we write $$\frac{12}{20}228 + \varphi^3 = 136.8 + 0.2360 = 137.0360 \quad (6)$$

we may interpret number 12 as the number of vertices of an icosahedron respectively number 20 as the number of faces of this regular polyhedron. In this way, the most important α constant of physics, besides the circle constant, is connected with the icosahedron and the golden mean, and also with the helix of life.
We can approximate the number 171 by the square of a golden number (see **Appendix** for *N* = 173), which is the infinitely continued fraction of number 13

$$13.07647321898^2 = \left(\frac{1}{0.07647321898}\right)^2 = 170.9941516 \quad (7)$$

The icosahedron equation maps for instance the positions of the face centers of an icosahedron with unit in-radius projected onto a complex plane where *z* is the coordinates [10]

[11] [12] [13]. Instead of following *Klein*'s quintic icosahedral solution, the substitution of the complex variable $z^5 \to x$ formally leads to a quartic polynomial

$$H(z,1) = z^{20} - 228z^{15} + 494z^{10} + 228z^5 + 1 \tag{8a}$$

$$H(x,1) = x^4 - 228x^3 + 494x^2 + 228x + 1 \tag{8b}$$

The roots accordingly correspond to the locations of the face midpoints on the *Riemann* sphere. Remarkable is the following representation of the icosahedron coefficients by *Fibonacci* number 13 [14] [15], which is a frequent protofilament number of helical structures and takes a formative role in life creation

$$\left(13 + \tfrac{1}{13}\right)^2 = 171.0059 \ldots \quad \tfrac{4}{3}\left(13 + \tfrac{1}{13}\right)^2 = 228.0078 \ldots \tag{9}$$

Then we can recast $H(x,1)$ yielding

$$H(x,1) \approx x^4 - \tfrac{4}{3}(13 + \tfrac{1}{13})^2 x\left(x^2 - \tfrac{13}{6}x - 1\right) + 1 \tag{10}$$

The four roots of this polynomial have been calculated giving

$$x_2 = -\frac{1}{x_1}, \quad x_4 = -\frac{1}{x_3} \tag{11}$$

$$x_2 = 2.58365039 \approx 228 - \tfrac{4}{3}13^2 = 2.66666 \tag{12}$$

$$x_4 = 225.80782741 \approx \tfrac{4}{3}13^2 = 225.33333 \tag{13}$$

In addition, it yields $\sum_{i=1}^{4} x_i = 228$ (14)

Regarding *Fibonacci* number 13 further, the equation

$$\tfrac{4}{3}(x + x^{-1})^2 = 228 \tag{15}$$

can be recast into the depressed quadric polynomial equation

$$x^4 - 169x^2 + 1 = 0 \tag{16}$$

with solutions $x_{1,2} = \pm\, 12.99977241 \approx \pm\, 13$ (17)

and $x_{3,4} = \pm\, {x_{1,2}}^{-1} = \pm\, 0.076924423 = \pm \frac{1}{12.99977241} \approx \pm \frac{1}{13}.$ (18)

The reader is frequently confronted with the *Fibonacci* number 13, which obviously plays an important role besides φ and φ^5 when assessing bio-coding and related storage and processing of information. Especially relation (8) as approximate icosahedron quartic points to reciprocity behavior of icosahedral structures.

In the following we will develop a system of interrelations to indicate the strong coupling between geometry and fundamental numbers as the corset of life and cosmic circumstances, thereby understanding, how self-organization in nature works. We begin with mass constituents of the universe and end with life and consciousness. Finally, we pose the question whether charge can simply be understood as friction on the vacuum condensate and whether the vacuum condensate has an almost regular structure.

3. Golden Mean and Its Fifth Power

First we must deal with the fifth power of the golden mean. We know that it governs phase transitions from particle to cosmic scale [16] [17] [18] [19]. The fifth power of the golden mean φ has the second simplest infinitely continued fraction representation besides that for the golden mean itself. We present an excerpt from the present author's publication [20]

$$\varphi = \frac{\sqrt{5}-1}{2} = \frac{1}{1+\frac{1}{1+\frac{1}{1+\cdots}}} = 0.618033989\ldots \qquad \Phi = \frac{\sqrt{5}+1}{2} = 1+\varphi \tag{19}$$

$$\varphi^3 = \frac{\sqrt{20}-4}{2} = \sqrt{5}-2 = \frac{1}{4+\frac{1}{4+\frac{1}{4+\cdots}}} = 0.236067977\ldots \tag{20}$$

$$D_{KK} = 5 + \frac{1}{4+\frac{1}{4+\frac{1}{4+\cdots}}} = 5 + 0.236067977\ldots \tag{21}$$

fractal part of *Kaluza-Klein* dimension D_{KK}

$$\varphi^5 = \frac{\sqrt{125}-11}{2} = \frac{1}{11+\frac{1}{11+\frac{1}{11+\cdots}}} = 0.0901699\ldots \tag{22}$$

$$\varphi^{-5} = 11 + \varphi^5 = 11 + \frac{1}{11+\frac{1}{11+\frac{1}{11+\cdots}}} = 11.0901699\ldots \tag{23}$$

fractal representation of the dimension in *Witten*'s M-theory.

Further details with respect to golden numbers can be obtained in the **Appendix**.

An interesting mathematical puzzle to solve is the sequence of only two numbers that results from taking the sixth root of the most irrational number φ

$$\sqrt[6]{\varphi} = 0.922929922\ldots \approx \frac{12}{13} - \frac{1}{3\cdot(3+\varphi)^6} = 0.9229283\ldots \tag{24}$$

The known series representation for φ can be applied more generally with some new didactic insights. It delivers

$$\sum_{n=1}^{\infty}\varphi^n = \sum_{n=1}^{\infty}\left(\frac{1}{\Phi}\right)^n = \varphi + \varphi^2 + \varphi^3 + \cdots = 1+\varphi = \Phi \tag{25}$$

If we use the reciprocal of the sum we get

$$\left(\sum_{n=1}^{\infty} \varphi^n\right)^{-1} = \varphi \tag{26}$$

Now we generalize this equation for positive real numbers

$$\left(\sum_{n=1}^{\infty} m^{-n}\right)^{-1} = m - 1 \tag{27}$$

As an important example we apply this equation for the interesting *Fibonacci* number $m = 13$

$$\left(\sum_{n=1}^{\infty} \left(\frac{1}{13}\right)^n\right)^{-1} = 12 \tag{28}$$

Summing only over uneven numbers $n = 1,3,5, \ldots$ we yield

$$\left(\sum_{n=1,3,5\ldots}^{\infty} \left(\frac{1}{13}\right)^n\right)^{-1} = 13 - \frac{1}{13} \tag{29}$$

or general for all positive real numbers

$$\left(\sum_{n=1,3,5\ldots}^{\infty} m^{-n}\right)^{-1} = m - \frac{1}{m} \tag{30}$$

The change from $m - \frac{1}{m}$ to $m + \frac{1}{m}$ can be performed by the relation

$$\left(m + \frac{1}{m}\right)^2 = 4 + \left(m - \frac{1}{m}\right)^2 \tag{31}$$

Another simple approximation connects the fifth power of the golden mean with reciprocal terms of number 13

$$\frac{\varphi^5}{1+\varphi^5} = \frac{1}{12+\varphi^5} = 0.0827118 \approx \frac{1}{13} + \frac{1}{13^2} = 0.082840235 \tag{32}$$

We work also with *Guinn*'s pioneering matter and space approach and with the maximum galactic velocity β_g [21]. Surprisingly, a paradigmatic reciprocity relation can be formulated using $\alpha^{-1} = 137.03599 \ldots$ [22] [23]

$$\pi \cdot |\beta_g| \approx \frac{1}{\pi \cdot \alpha^{-1}} \tag{33}$$

This is the real mystery behind number 137, if any mystery can be seen at all. It may be considered as a signature of matter-wave duality and galactic entanglement. Other approximate relations exist between powers of the golden mean and *Guinn*'s galactic velocity β_g [21]

$$\varphi^5 = 0.090169987 \approx \sqrt[3]{|\beta_g|} = 0.0904274 \tag{34}$$

$$\varphi^6 \approx 24 \cdot \sqrt{\alpha \cdot |\beta_g|} = 0.05574998 \tag{35}$$

The maximum velocity $\frac{v_m}{c} = \beta_m$ of the difference curve between rotation velocity and precession velocity according to *Guynn* [21] can be approximated by golden mean based quantities or π based ones, remembering that φ^5 is the maximum of the *Hardy-Suleiman* relation [17] [18] [19], before used by *El Naschie* in his ε-infinity theory [24] [25] [26]. Both numbers φ and π are related to each other, for instance see relation (1). One can confirm the following approximations

$$\frac{v_m}{c} = \beta_m = \sqrt{3} \cdot \left(\sqrt[3]{2} - 1\right) = 0.450196459 \ldots \tag{36}$$

$$\approx \frac{\sqrt{2}}{\pi} = 0.450158158\ldots \tag{37}$$

$$\approx 5 \cdot \varphi^5 = 0.4508497 \ldots \tag{38}$$

$$\approx \frac{3}{2} \cdot \sqrt{\varphi^5} = 0.450424549 \ldots \tag{39}$$

Interestingly, the factor $\sqrt[3]{2}$ in relation (36) represents the *Lorentz* factor for the maximum difference velocity between rotation angular velocity and precession angular velocity in *Guynn*'s seminal structure and matter approach [21] [4]. This special *Lorentz* factor $\gamma_1$can be approximated well by a relation that shows the fifth power of the golden mean:

$$\gamma_1 = \sqrt[3]{2} = 1.25992105 \ldots \approx 1 + \frac{5\varphi^5}{\sqrt{3}} = 1.2602982 \ldots \tag{40a}$$

Furthermore, connecting γ_1 with the dihedral angle of a regular icosahedron leads to the simple relation

$$\gamma_1 - 1 \approx \frac{\sin(138.189251)}{\pi} \tag{40b}$$

When connecting γ_1 with its reciprocal we get again a golden mean approximation

$$\gamma_1 + \frac{1}{\gamma_1} = 2.053613787 \approx \varphi^{-\frac{3}{2}} = 2.058171 \tag{41}$$

Further, with reference to equation (36) we may ask how the fifth power of the golden mean φ^5 is connected with $\gamma_1^2 = \sqrt[3]{4}$? Again we combine this term with its inverse value and get

$$\sqrt[3]{4} + \frac{1}{\sqrt[3]{4}} = 2.21736157 = \frac{1}{0.450986438} \approx \frac{1}{5 \cdot \varphi^5} = \frac{1}{0.450849935} \tag{42}$$

The quadratic equation $$x^2 - \left(\sqrt[3]{4} + \frac{1}{\sqrt[3]{4}}\right) \mathrm{x} + 1 = 0 \tag{43}$$

has the two solutions $$x_1 = \sqrt[3]{4}, \quad x_2 = 1/\sqrt[3]{4} \tag{44}$$

Again we can approximate the circle constant π by

$$\pi \approx 2 \cdot (\gamma_1^2 + \gamma_1^{-2}) = 3.1358 \ldots \tag{45}$$

4. Gyromagnetic Factor of the Electron

The anomalous gyromagnetic factor of the electron was recently calculated very precisely without any *QED* construct by *Preston Guinn* [21]. Besides this famous result our less precise fractal attempt of the anomalous part based solely on the golden mean may be given here [7]

$$g_e \approx 2 + \frac{1}{2}\left(1 + \frac{\varphi^6}{24} - \frac{1}{1+\frac{\varphi^6}{24}}\right) = 2.002319313\ldots \tag{46}$$

$$g_e \approx 2 + \frac{\varphi^6}{24} - \frac{1}{2}\left(\frac{\varphi^6}{24}\right)^2 - \frac{1}{4}\left(\frac{\varphi^6}{24}\right)^3 = 2.002319304\ldots \tag{47}$$

where the denominator $24 = 2 \cdot 12$ may be a hint to the icosahedral ball structure of the electron [7]. Interestingly, the in-sphere volume of a regular icosahedron is proportional to $1/\varphi^6$ [27], and

$$\frac{\varphi^6}{24} \approx \sqrt{\alpha|\beta_g|} \tag{48}$$

This result may be compared to the high accuracy of the best known experimental value for g_e determined as one-electron cyclotron transition for an electron trapped in an electrostatic quadrupol potential (*Penning* trap) [28]

$$g_e = 2.00231930436182(52) \tag{49}$$

5. Hardy-Suleiman Function

Hardy's maximum quantum entanglement probability of two quantum particles [17][18] exactly equals the fifth power of φ. This asymmetric probability distribution function P with p_τ as entanglement variable, running from not entangled states to completely entangled ones, is given by

$$P = p_\tau^2 \, \frac{1-p_\tau}{1+p_\tau} \tag{50}$$

Hardy's quantum probability function of two particles was investigated in more detail and connected with results of mathematical statistics and statistical mechanics [17] [18]. This function, displayed in **Figure 1**, turns out to be a central topic of the *Information Relativity* theory of *Suleiman* [16] [17] by mapping the transformation of his relative energy density. The maximum of the energy density relation at a recession velocity of φ yielded exactly φ^5 and was attributed to criticality of a transition at cosmic scale [16] [19]. An excellent polynomial approximation for the *Hardy* function respectively the *IRT* matter energy density was given by the present author, where $x = \beta = \frac{v}{c}$ is the recession velocity [29].

$$\tilde{h}(x) \approx \sum_{n=1}^{\infty} x^2 \cdot \left(\frac{1-x}{2}\right)^n = x^2\left(\frac{(1-x)}{2} + \frac{(1-x)^2}{4} + \frac{(1-x)^3}{8} + \frac{(1-x)^4}{16} + \frac{(1-x)^5}{32} + \cdots\right). \tag{51}$$

In **Figure 1** the *Hardy* function is compared with its power series expansion summed up only to the fifth term. However, when replacing a symmetric double well by an asymmetric curve

involving the fifth power of the golden mean as coefficient $(1+\varphi^5)$ of the quadratic term according to

$$q(x) = x^4 - 2x^3 + (1+\varphi^5)x^2 \tag{52}$$

then *Hardy*'s functions can be well approximated still beyond the local maximum exactly located at $x = \varphi$. Interestingly, the coefficient of the quadratic term contains the fifth power of the golden mean, which is by the same time the value of the local maximum at $x = \varphi$ and also the value at $x = 1$.

Recently, we compared the matter and space approaches of *Suleiman* and *Guynn* [30]. We recast *Suleiman*'s matter energy density formula $h(x)$ [3]

$$h(x) = x^2 \cdot \frac{1-x}{1+x} = x^2 \cdot \frac{(1-x)^2}{(1+x)(1-x)} = x^2(1-x)^2\gamma^2 \tag{53}$$

Then we can simply write down the square root of this formula using the Lorentz factor γ

$$f(x) = \sqrt{h(x)} = x(1-x)\gamma \tag{54}$$

The function $f(x)$ has a maximum value of $y_m = \sqrt{\varphi^5}$ at $x_m = \varphi$. Whereas *h(x)* represents the energy density, *f(x)* is proportional to a speed and can be compared with *Guynn*'s formula for the difference speed after coordinate transformation and simplification [30].

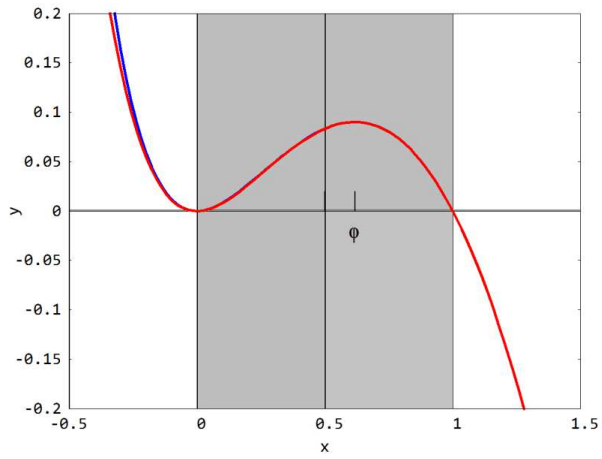

Figure 1. Comparison of *Hardy* function (blue) with its polynomial expansion (red). Only the first 5 terms are use as given in relation (51).

6. Mass Constituents of the Universe

If we keep the hierarchy of the fifth power of the golden mean respectively *Guynn*'s galactic velocity [16] involved in the inflation of the constituents Ω_i of the universe (*M* baryonic matter, *DM* dark matter, *DE* dark energy), then we can write down surprisingly simple the next three relations, where β_m is the maximum galactic difference velocity

$$\frac{\Omega_M}{\Omega_{DM}} \approx 2 \cdot \varphi^5 \approx \frac{2}{5}\beta_m \tag{55}$$

$$\frac{\Omega_M+\Omega_{DM}}{\Omega_{DE}} \approx 5 \cdot \varphi^5 \approx \beta_m \tag{56}$$

$$\frac{\Omega_{DM}}{\Omega_{DE}} = 0.3924 \approx \frac{5\sqrt{3}}{2}\varphi^5 = 0.390447 \approx \frac{\pi}{8} \approx \frac{\sqrt{3}}{2} \cdot \beta_m = 0.39988 \approx \frac{2}{5} \tag{57}$$

Interestingly, the quotient of baryonic matter to total matter is again related to the golden mean respectively to β_0

$$\frac{\Omega_M}{\Omega_M+\Omega_{DM}} = \frac{\Omega_M}{1-\Omega_{DE}} = 0.1545 = \frac{0.6183}{4} \approx \frac{\varphi}{4} \approx \frac{1-\beta_0}{\beta_0} \tag{58}$$

where $\beta_0 = \frac{v_0}{c} = \frac{\sqrt{3}}{2}$ is the velocity, at which the difference between galactic rotation velocity and *Thomas* precession is equal [21]. What means such a numerical relationship between the mass constituents? It confimes that these quantities aren't independent from each other and may develop in cosmic times.

Now we start with *Bouchet*'s mass constituents summarized in **Table 1** [31] [32] together with our recent calculations [30] and present cubic polynomials

$$P(x) = ax^3 + bx^2 + cx + d \tag{59}$$

derived from 4 points with coordinates given in **Table 2**. Each coordinate point number 3 serves, besides the origin, as a golden mean based fixpoint. These fixpoints can be related to the maxima of the matter energy density according to the *IRT* theory [16] [19]. The fixpoints sum up to unity (see **Figure 2**). What we get is a number-theoretical reciprocity chamemeon of the golden mean imprinted on the mass constituents of our Universe. **Figure 2** illustrated the relationship between the polynomials and the golden mean hierarchy.

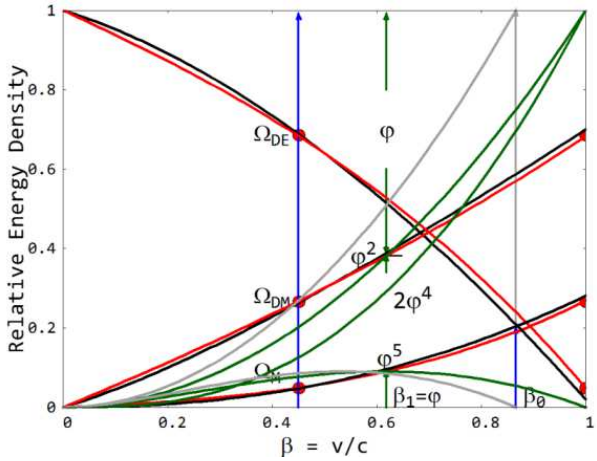

Figure 2. Illustration of the polynomial representation of mass constituents as red curves with inverse values generated at $\beta = 1$. Black curves represent relations given in the **Appendix**, green curves display energy densities according to the *IRT* theory [19], grey curves have been generated from the green ones by replacement of β by β/β_0, where $\beta_0 = \sqrt{3}/2$ [21], Ω_i = mass constituents.

The situation, where the mass constituents change their values, may be characterized as a phenomenon or chameleon not yet fully understood that gives a hint of a cyclic universe. Again the phenomenon of reciprocity relations is addressed here.

Table 1. Mass Respectively Energy Constituents of the Universe

Constituent	***WMAP*** [32]	**Calculation** [33]	
		β_m conjecture	φ conjecture
Ω_M	0.049	0.04579	0.04852
Ω_{DM}	0.268	0.26613	0.26756
Ω_{DE}	0.683	0.68808	0.68392
$\Sigma\Omega_i$	1.000	1.00000	1.00000

Table 2. Coefficients of the Cubic Polynomials $P(x) = ax^3 + bx^2 + cx + d$

Coefficients	**Polyomial 1**	**Polynomial 2**	**Polynomial 3**
a	0.17677	0.05263	1.18261
b	0.03365	0.08489	-2.16718
c	0.05758	0.54545	0.03357
d	-	-	1
P(1)=a+b+c+d	0.26800	0.68297	0.0490

Table 3. Coordinates For Generating Cubic Polynomials

Points	***x***	**y**
	Polynomial 1	
1	0	0
2	$5\varphi^5$	Ω_M
3	φ	φ^5
4	1	Ω_{DM}
	Polynomial 2	
1	0	0
2	$5\varphi^5$	Ω_{DM}
3	φ	φ^2
4	1	Ω_{DE}
	Polynomial 3	
1	0	1
2	$5\varphi^5$	Ω_{DE}
3	φ	$2\varphi^3$
4	1	Ω_M

7. Duality between Volume and Surface

In this Chapter we report mass constituents of the universe concluded from the duality between volume and surface. However, these values are numerically not so convincing compared to the last experimental values [32] as values obtain in Chapter 6. The relationship between volume and surface goes far beyond a purely geometric understanding. The duality between volume and surrounding surface respectively between any compact entity and assigned surface in general as well as the duality between a moving particle respectively body and the accompanying wave or reciprocity between matter and dark matter is the very spice of life. It has been impressively formulated by the words of *Nobel* laureate *Wolfgang Pauli*: "God made the bulk; surfaces were invented by the devil" (quoted from [34]). Nature used to compact matter in special volumes, for instance in icosahedral bodies as proposed for the chiral electron 'ball' structure [7] respectively folded chiral DNA strings in icosahedral virus structures. Because the starting entities have both chiral properties, the compaction consequently leads to chiral bodies. Chirality plays also an important role in the next chapter. Seemingly the entire universe is chiral.

El Naschie's E-infinity (ε^{∞}) theory [35], not commonly known or accepted by physicists, originates from a fractal *Cantorian* set theory [36] as a number-theoretical route of physics for explaining the dualism between particles and waves that can help solving cosmological mysteries such as dark matter and dark energy [37]. The quantum particle P_Q is symbolized by the bi-dimension of the zero set, while the guiding wave W_Q surrounding the quantum particle is given by the bi-dimension of the empty set according to

$$dim(X) = (n, d_c^{(n)}) \tag{60}$$

where *n* is the *Urysohn-Menger* topological dimension [38][39] and

$$d_c^{(n)} = (\varphi^{-1})^{n-1} \tag{61}$$

represents the *Hausdorff* dimension [40], where φ is the golden mean as defined before.

It results for P_Q $$dim(P_Q) = (0, \varphi), \tag{62}$$

respectively for W_Q $$\dim(W_Q) = (-1, \varphi^2) \tag{63}$$

By using these dimensions a probabilistic quantum entanglement calculation with velocity restriction $v \to c$ delivers effective quantum gravity formulas for the cosmological mass (energy) constituents as follows [25] [41] [42]

$$\Omega_M = \frac{1}{2}\frac{(1-\varphi)}{(1+\varphi)}\varphi^2 = \frac{\varphi^5}{2} = 0.04508497 \approx \frac{\pi-3}{\pi} \tag{64}$$

$$1 - \Omega_M = \frac{5}{2}\varphi^2 = 0.9549150 \tag{65}$$

$$\Omega_{DM} = \frac{3}{2}\varphi^4 = 0.218847 \tag{66}$$

$$\Omega_{DE} = 2\varphi - \frac{1}{2} = 0.736068 \tag{67}$$

$$\Sigma\Omega_i = 1 \tag{68}$$

Recasting the matter amounts into a suitable form,

$$\Omega_M = \frac{1}{10}5\varphi^5, \qquad \Omega_{DM} = \frac{1}{10}(5\varphi^5)^{-1} = 0.2218 \tag{69}$$

a reciprocity relation was confirmed between Ω_M and Ω_{DM} giving a persuasive equation for the pure dark energy [41]

$$\Omega_{PD} = 1 - \frac{1}{10}\,(5\varphi^5 + (5\varphi^5)^{-1}) = 0.7331\ (73.31\%) \tag{70}$$

Such quantum entanglement based coincidence means that the constituents of the cosmos should not be considered independent of each other, which was confirmed by the information relativity theory (*IRT*). Importantly, if one compares the results given here with the following ones of the information relativity theory, then *El Naschie*'s set theoretical approach is restricted to $v \to c$, whereas the more general *IRT* theory delivers results for the recession velocity $\beta = \frac{v}{c}$ in the hole range $0 \leq \beta \leq 1$ (c is the speed of light).

8. Newly Introduced Numbers (Angles)

a) Fibonacci Net Angle α_F

Recently, two new numbers respectively angles were introduced from the present author with importance to life, physics and the cosmos [3]. The first angle was designated α_F. It can be derived from a *Fibonacci* net with 13 subunits in a hexagonal basis cell, offset by an angle of $\alpha_F = 13.898°$ (**Figure 3**). This net can be uprolled to a helical tubule with <$\mathbf{N}_{pf}$> = 13 'protofilaments' resembling the tubulin microtubule. Denominating the lattice parametr of the large cell as a and that of the sub-cell as a_{sub}, then between both parameters exists the relation

$$a_{sub} = \frac{a}{\sqrt{13}} \tag{71}$$

Notice that the sub-cell plane has *Miller* indices $(31\bar{4}0)$, where $h^2 + k^2 + hk = 13$.
The angle α_F between sub-cell direction and *a*-axis can be calculated as

$$\alpha_F = arctan\left(\frac{5}{3\sqrt{3}}\right) - 30 = 13.897886° \tag{72}$$

When the starting small cell is helically wound at the twist angle of α_1, it needs 13-times the small cell lattice parameter a_{sub} to reach again identity with a large cell lattice point. By a full turn one gains a height in filament direction of

$$h_{13} = \frac{\sqrt{3}}{2}a = \frac{\sqrt{39}}{2}a_{sub} \approx \pi \cdot a_{sub} \tag{73}$$

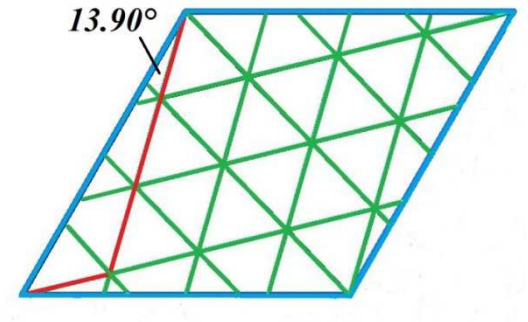

Figure 3. *Fibonacci* net composed of 13 triangular sub-cells offset by an angle of 13.9° in comparison to the blue outlined 'unit cell'

From a geometrical viewpoint the importance of protofilament number 13 may be manifested as a sort of frustration due to the almost identical angles between the *Fibonacci* net offset angle α and the angle $\alpha' = 180°/13$ of the base circle

$$\alpha_F = 13.898° \approx 4\pi + \frac{\pi+1}{\pi} = 13.88468 \approx \alpha' = \frac{180^\circ}{13} = 13.846° \tag{74}$$

Furthermore it yields $$\frac{\sin(\alpha_F)}{\pi} = 0.0764561 \approx \frac{1}{13+\frac{1}{13}} = 0.076470 \tag{75}$$

and $$\sin(13.8863) = 0.2399959 \approx \frac{\pi}{13+\varphi^5} = 0.2399963 \tag{76}$$

Interestingly, the out-sphere diameter of an icosahedron of edge length a is

$$\sqrt[4]{13+\varphi^5} \cdot a = 1.90211 \cdot a \approx \sqrt[4]{13+\frac{1}{13}} \cdot a = 1.90163 \cdot a \tag{77}$$

respectively $$\approx \sqrt[4]{\pi(\pi+1)+\frac{1}{\pi(\pi+1)}} \cdot a = 1.90203 \cdot a \tag{78}$$

We may compare this result with the roots of the depressed quartic polynomial

$$x^4 - (\frac{n}{a} - 2)\, x^2 + 1 = 0 \tag{79}$$

which can easily be calculated by the relation

$$x_i = \pm\sqrt{\frac{n}{2a} - 1 \pm \sqrt{\left(\frac{n}{2a} - 1\right)^2 - 1}} \tag{80}$$

with the result $x_{3,4} = \pm x_1^{-1}$. For $n = 173$, $a = 1$ we obtain

$$x_1 = 13.07647321898 \tag{81}$$

$$x_3 = x_1^{-1} = 0.07647321898 \tag{82}$$

$$x_1{}^2 = 170.99415\ldots \tag{83}$$

$x_1 = 13.07647321898$ represents a golden number. However, x_3 is also the result of the infinitely continued fraction representation applied to number 13 [20].

$$\frac{1}{13+\frac{1}{13+\frac{1}{13+\cdots}}} = 0.076473218\ldots \tag{84}$$

We already connected the term $\frac{1}{13+\frac{1}{13}}$ with icosahedron mathematics as well as the following relation

$$\frac{4}{3}\left(\frac{\pi}{\sin(13.900)}\right)^2 = 228 \tag{85}$$

We used such relations in our approach of the icosahedral *Moebius*-ball electron and in the formula for the gyromagnetic factor of the electron [14]. The fractal part of the gyromagnetic factor of the electron can be given as

$$\Delta g_e = \left(\frac{2}{3\cdot\alpha_F}\right)^2 = 0.00231930436 \tag{86}$$

when exactly using $$\alpha_F = 13.8429888 \tag{87}$$

From *Sommerfeld*'s inverse structure constant α^{-1} we get the angle α_F

$$\alpha_F \approx \frac{2}{3}\sqrt{\pi\alpha^{-1}} = 13.8325 \tag{88}$$

$$\alpha_F \approx \frac{4\pi}{3}\frac{1}{e}\sqrt{\varepsilon_0\bar{h}c} \tag{89}$$

where e is the electron charge, $\bar{h}$ is the reduced *Planck* constant and c is the speed of light. Indeed, the angle α_F seems to be of fundamental importance for geometry, life science and physics, remembering

$$\alpha_F \approx \frac{180}{13} = 13.84615\ldots \tag{90}$$

Using equation (73) one can formulate a mathematical gimmick

$$\left(\frac{2}{3\cdot\frac{180+\Delta}{13}}\right)^2 = \Delta \tag{91}$$

with the result $\Delta = 0.002318184$ ...

Turning back to a helix with 13 protofilaments, we are now interested in the relation between the volume and surface. **Figure 4** below displays a projection of a constructed <$\mathbf{N}_{pf}$> = 13 microtubule down its filament axis.

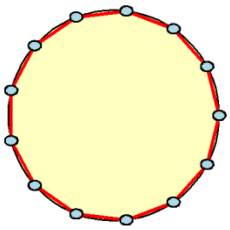

Figure 4. Helically twisted microtubule projected down the filament direction with 13 light-blue atoms or atom groups on sub-lattice positions.

We can use the outer diameter represented by the black line or the inner diameter as tangent to the projected red subunit a_{sub}. We get for the volume V

$$V_i = \pi \cdot r_i^2 \cdot h_{13} = \pi \cdot (1 - \frac{3}{4\cdot 13}) \cdot \frac{\sqrt{39}}{2} \cdot \frac{1}{\tan^2(\frac{180}{2\cdot 13})} \cdot a_{sub}^3 \tag{92}$$

$$= \pi \cdot \frac{49}{8} \cdot \sqrt{\frac{3}{13}} \cdot \frac{1}{\tan^2(\frac{180}{2\cdot 13})} \cdot a_{sub}^3 \tag{93}$$

For the surface O_i without the circular covers we obtain

$$O_i = 2\pi \cdot r_i \cdot h_{13} = \pi \cdot 2\sqrt{(1 - \frac{3}{4\cdot 13})} \cdot \frac{\sqrt{39}}{2} \cdot \frac{1}{\tan(\frac{180}{2\cdot 13})} \cdot a_{sub}^2 \tag{94}$$

$$= \pi \cdot \frac{7}{2}\sqrt{3} \cdot \frac{1}{\tan(\frac{180}{2\cdot 13})} \cdot a_{sub}^2 \tag{95}$$

For the ratio V_i/O_i we obtain a remarkable reciprocity relation, which points again to the importance of protofilament number 13

$$\frac{V_i}{O_i} = \frac{7}{4\cdot\sqrt{13}} \cdot \frac{1}{\tan(\frac{180}{2\cdot 13})} \cdot a_{sub} \tag{96}$$

$$= \frac{13+1}{8\cdot\sqrt{13}} \cdot \frac{1}{\tan(\frac{180}{2\cdot 13})} \cdot a_{sub} = \frac{1}{8\cdot\tan(\frac{180}{2\cdot 13})} \cdot (\sqrt{13} + \frac{1}{\sqrt{13}}) \cdot a_{sub} \tag{97}$$

$$\approx (\sqrt{13} + \frac{1}{\sqrt{13}}) \cdot a_{sub} \tag{98}$$

Resume: **We have demonstrated the intimate connection between a 13-protifilament helix, the icosahedron and *Sommerfeld*'s structure constant *α*.**

b) Parent-Sibling Relation and Angle α_1

Recently, the concept of paired entities as nature's reproductive strategy was introduced and the dominance of golden mean solutions by simple mathematical assumptions verified including 'golden' quartic polynomials [43]. So the Split-Sphere-Volume concept was worked out. A new omnipresent magic angle around $\alpha_1 = 50.95°$ was documented connecting again life, physics and cosmos. This is the second important angle we present arising from a parent-sibling relation.

Following the concept of paired entities, we will split the volume of a parent sphere with unit radius into two smaller but equal spheres. Assuming constant density, the volume is proportional to mass and also to energy. Following **Figure 5**, interesting geometrical relations can be confirmed showing signature of the golden mean respectively its fifth power.

The starting sphere volume is denoted as V_0 and the half volume as V_1. Then we get the trivial results

$$V_0 = 2 \cdot V_1 \tag{99}$$

$$V_0 = \frac{4}{3}\pi r_0^3 \tag{100}$$

$$V_1 = \frac{V_0}{2} = \frac{4}{3}\pi r_1^3 = \frac{4}{3}\pi \left(\frac{r_0}{\sqrt[3]{2}}\right)^3 \tag{101}$$

$$\cos(\alpha_{1)} = \frac{r_0}{2r_1} \tag{102}$$

$$\alpha_1 = 50.9527898° \tag{103}$$

$$\frac{\alpha_1}{360} = 0.141535527 \approx \pi - 3 = 0.141592653 \tag{104}$$

$$\frac{\alpha_1}{180} = 0.28307105 \approx \pi \cdot \varphi^5 = 0.283277231 \tag{105}$$

$$h_1 = 0.61640938 \cdot r_0 \approx \varphi \cdot r_0 \tag{106}$$

where $\varphi = \frac{\sqrt{5}-1}{2} = 0.6180339887$ is the golden mean. If we change only marginally the sphere radius ratio, then exact golden mean solution for instance to relation (49) can be obtained using $V_0 = 1.99521 \cdot V_1$ instead of $V_0 = 2 \cdot V_1$. Clearly, surface energy should play a role besides volume energy. **Table 4** in the **Appendix** shows summarized intrinsic geometric frustrations around the α_1 angle related to the split sphere volume approach.

We note that the following relation holds too (see **Table 4**)

$$\arctan(2\varphi) = 51.026552° \tag{107}$$

We can both new angles relate to each other by multiplication with a quotient

$$\frac{11}{3} \cdot 13.897886° = 50.958916° \tag{108}$$

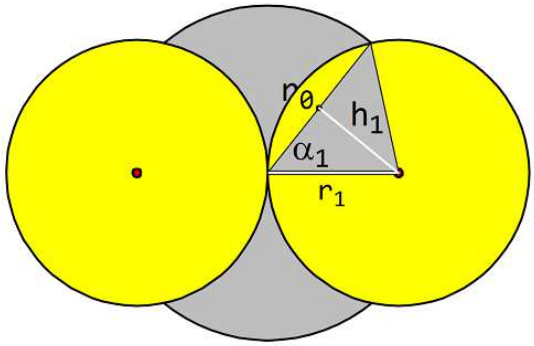

Figure 5. Splitting of a parent sphere (red) into two spheres each with half volume (yellow)

The angle α_1 can also be derived from the following simple relation

$$\alpha_1 = \pi^2 \cdot \varphi^5(rad) \widehat{=} 50.9899° \tag{109}$$

The importance of the angle α_1 can be underlined by the following simple relation with respect to the mass m_{Hi} of the *Higgs* boson, which is seemingly a paired entity [44]

$$m_{Hi} = \frac{\alpha_1}{\varphi^2}\left(m_p + m_e\right) = 125.23\ GeV/c^2 \tag{110}$$

where m_p is the mass of the proton respectively m_e the mass of the electron. The fundamental character of the magic α_1 angle may be indicated by the recast mass quotient relation using the precisely determined *Higgs* boson mass of 125.22 GeV/c^2 [45]

$$\alpha_1 = \varphi^2 \frac{m_{Hi}}{m_p + m_e} = 50.94871° \tag{111}$$

The number $\frac{\alpha_1}{\varphi^2}$ can be related to *Dirac*'s large number (*DLN*) [46]

$$\sqrt[20]{\frac{10^{43}}{\pi}} = \sqrt[20]{DLN} \approx \frac{\alpha_1}{\varphi^2} = 133.3959128 \tag{112}$$

This number is found by the following relation given by *Kosinov* [47] as the geometric mean between the reciprocal *Sommerfeld* constant and the number for small distances $N_{sd} = 129.85250805$, which is related to *Dirac*'s large number

$$\sqrt{\alpha^{-1} \cdot N_{sd}} = 133.3959128 \tag{113}$$

c) Another Magic Angle α_m

Another 'magic' angle α_m is related to α_1 and can be derived from the following relation using the integral of the *Lorentz* transform [15] [48]

$$\int_0^{\varphi^5} \frac{1}{\sqrt{1-\beta^2}}\, d\beta = \arcsin(\varphi^5)\,(rad) \mathrel{\widehat{=}} 5.173386° = \alpha_m \tag{114}$$

$$\alpha_m{}^{\circ} \cdot \pi^2 = 51.05927° \tag{115}$$

This new angle can also be related to α_F

$$\frac{72}{5.173386} = 13.91738 \approx \alpha_F \tag{116}$$

Interesting is also the vicinity of this angle to the result of the infinitely continued fraction of number 5

$$\cfrac{1}{5+\cfrac{1}{5+\cfrac{1}{5+\cdots}}} = 0.192582403\ldots \tag{117}$$

The inverse of the result is the golden number 5.19258240…

Thus we can relate the angles to each other in full glory

$$\boldsymbol{\pi^2 \approx \frac{\alpha}{|\beta_g|} \approx \frac{\alpha_1}{\alpha_m} \approx \frac{\alpha_1 \cdot \alpha_F}{72}} \tag{118}$$

9. Geometric Frustration

The very significance of geometrical frustration was recognized first by *Linus Pauling* who had exemplarily evaluated the low temperature ordering of protons in crystalline ice [49] [50]. The entropy S_0 of a system can be derived from the effective number of ground states W (total number of ground states reduced by the action of constraints) according to the *Boltzmann* relation [51]

$$S_0 = k_B \cdot \ln(W) \tag{119}$$

The number of tetrahedrons in the ice structure counts $N/2$. Then the number of ground states can be calculated yielding

$$W = \left(\frac{3}{8}\right)^{N/2} \cdot 2^N \tag{120}$$

Finally, the renormalized entropy yields

$$\frac{S_0}{k_0 N} = \frac{1}{N}\ln(W) = \frac{1}{2}\ln\left(\frac{3}{2}\right) = 0.20273 \approx \frac{2}{\pi^2} = 0.20264 \tag{121}$$

We have added to this result a π-based approximation for further considerations about an extended approach of geometrical frustration.
Now we turn to the α-helix peculiarities of proteins where 18 subunits perform 5 turns to reach an identical position when projected down the fiber axis [15] [10]. This means one needs per turn 3.6 subunits. This number is nearby another golden mean derived number

$$3 + \varphi \; = \; 3.6180339887 \ldots = \sqrt{13 + \varphi^5} = \sqrt{2 + \varphi^{-5}} \tag{122}$$

In case of the α-helix, when tentatively using 3.61803… subunits per turn instead of 3.6, one would end with $18 \; + \; \varphi^5$ subunits after 5 turns

$$5(2 + \varphi^{-1}) = (\varphi^5 + \varphi^{-5})\varphi^{-1} = 18 \; + \; \varphi^5 = 18.0901699 \ldots \tag{123}$$

and again the fifth power of the golden mean would be involved when the helix breathes a little bit. Solving the depressed quartic polynomial for number $n = 18^2 + 4 = 328$ (equation 15) we get similar but golden solutions with reciprocity properties, identical with the infinitely continued fraction representation of number 18

$$x_{1,2} = \pm 18.0553851 \qquad x_{3.4} = \pm 0.0553851 \tag{124}$$

The folding propensity of helices or double-helices, for instance *Pauling*'s α helix, is caused by *von der Waals* forces respectively the *Casimir* force [52] [53] rather than by a network of hydrogen bonds. Geometrical restrictions and relations between fundamental numbers dictate folding details. The strong relation beweeen fundamental numbers supports geometric frustration. Viral self-assembly adapting icosahedral symmetry requires two internal protein configurations [54] as is the case for quasicrystals that form rhombic triacontahedrons [27] [55]. Quasicrystals represent a geometrically frustrated system composed of two golden mean based subunits. The value of the configuration entropy S_{conf} of a hard-sphere quasicrystal that supports nano-scale self-assembly can therefore approximated by a relation of the fifth power of the golden mean or alternatively by a relation of *Fibonacci* number 13

$$\frac{S_{conf}}{Nk_B} \approx \frac{\varphi^5}{1+\varphi^5} = \frac{1}{\varphi^{-5}+1} = \frac{1}{12+\varphi^5} = 0.08271 \approx \frac{1}{13} + \frac{1}{13^2} = 0.08284 \tag{125}$$

$$\approx \frac{(\pi-3)}{(\pi-3)+\frac{\pi}{2}} = 0.082687 \tag{126}$$

In the **Appendix** the reader can find a golden number result as approximation for the value given above, which is the infinitely continued fraction of number 12

$$0.08276253 = \frac{1}{12.08276253} \tag{127}$$

One may also remember that the sum of potencies of $\frac{1}{13}$ is $\frac{1}{12} = 0.0833333$ (equation 20).
Why are the ideas posed important? Because frustration and reversibly nested self-assembly of organic entities may be requisites for a possible artificial creation of life. Support of such

reversible processes can be given by a toggle switch operated by a very small magnetic or electric field. Nature use every now and then magnetic minerals.

10. Vacuum Energy Field

Postulating that an vacuum energy condensate exists, the gravity can be explained by displacement of this field by massive bodies [56]. A recent work by *Markoulakis* about the superluminal graviton condensate vacuum deserves our full attention [57]. The enormous speed of the postulated oscillating superluminal graviton string-particle of $v_{vac} \approx 10^{22} \cdot c$ as calculated by *Markoulakis* [57] points to "apparent" non-locality effects, obviously observed as practically instantaneous action at a distance in quantum entanglement experiments. This result strongly supports the **I**nformation **R**elativity **T**heory (*IRT*) of *Ramzi Suleiman*, which is indeed a local theory of matter and energy and as such as yet not accepted by mainstreamers [19]. Nothing is still known about whether light quanta twitch on such expected (icosahedral) vacuum energy grid thereby having much greater speed sideway than measured as forward component *c*. We pose another question about the origin of charge. Charge of opposed sign is created, when a high-energy photon is rapidly stopped at a solid barrier and decomposes into helically curled elecron and positron. Thereby work is done against the vacuum condensate energy field. However, the electric charge get the emerging particles beeing couples furthermore, of course depending on the distance between them. Speaking in philosophical parlance, matter including particles may emerge as compacted protuberances from this vacuum condensate network like mushroom fruiting bodies sproutinh from a fungal network.

11. Memory and Consciousness

The ability of living creations to store and process a huge amount of information with extremely high speed is connected with an extended chiral network of folded helically curled molecular chains with holographic property, in whose energy sinks and channels *Weyl* fermion pairs nest. Historically, the early theory for such fermions was worked out by *Hermann Weyl* already in 1929 [58]. In 1937, *Conyers Herring* supposed the existence of *Weyl* fermions in condensed matter [59]. Finally in 2015, *Weyl* fermions have been discovered in semimetals independently by different research teams [60] [61]. Whereas the photon is considered to be composed of helices of opposed chirality, *Weyl* fermions exist as such composite excitation with significantly distanced opposite helices in acentric domains. The displacement or activation of *Weyl* fermion pairs would lead to dissipationless high-speed information writing, storage or read out. One may not rule out that also superconductivity is involved in processes of information processing [62] [63]. Even water helices in helical tube scaffolds are expected to become superconducting at ambient conditions [64] [65]. However, the outlined fundamental properties of geometry and stochastics are ever behind such processes of information processing, which ability of living creatures was evolved through repeated mutation, selection and adaption.

In 1921 *P. P. Ewald* introduced an approach to determine quite convergent electrostatic lattice potentials (*Madelung* potentials) by a method that used real space besides reciprocal space calculations [66]. We should check whether our brain could profitably use such a method of information processing by combining direct pictures and diffracted ones. In this way, data loss could be avoided quite effectively. Such an approach is also conceivable for computer

applications. At the end it is most likely that information can superluminally travel along lines of the vacuum condensate energy field.

12. Superconductivity

We associated before phase transitions and superconductivity with the fundamental number of φ^5 that for the first time insinuate superconductivity being a property of energy fields of cosmic scale [16] [67]. Nowadays researchers connect superconductivity with the properties of the all-pervading *Higgs* field, where the associated fundamental *Higgs* boson represents an oscillating excitation of this field [68] [69] [70]. The basic idea to associate superconductivity with the *Higgs* field properties come from leading researchers many years ago [71] [72] [73] [74].

The charge-neutral *Higgs* mode collective oscillation of superconductors represents the condensed-matter analog of a *Higgs* boson [68] [69] [70]. The elusive *Higgs* particle with zero spin could indeed be a composite particle like the *Cooper* pair. The effective mass of such a composite can be marginally higher than the mass of the particle sum as was recently experimentally verified for a *Cooper* pair giving $2m_{eff} = 1.00084 \cdot 2m_e$ [75]. When multiplying the m_H value with this factor together with the factor given in relation (74), we get a value of m_{Hi} very near to its experimental value. However, if we conjecture that superconductivity is caused exclusively by holes and hardly by electrons, an exciting insight first postulated by *Hirsch* [76], then we must work with the effective hole mass. Could the *Higgs* boson by analogy with *Hirsch*'s assumption be related to any paired holes of matter? Pairing is the very essence of our existence. Following such 'pairing law', invisible hole pairs of heavy effective mass could constitute the energy field and medium that allows any waves to travel. The speed of light, for instance, should depend on the hole pair density. Remembering, the photon can be decomposed into a couple of electron – positron fields. When asking, what the structure of delocalized hole-carriers in the superconducting state would be, as all-convincing test case of our approach, the assumed chiral *Moebius* stripe governed property of the single electron could be relevant. A delocalized electron hole may also be portrayed by a helical strand able to transport positive charge. During the unfolding of involved delocalizing *Moebius* electron balls a nested double-helical wavy entity of equal strand chirality (*DNA* case) could be formed, which can easily be unzipped just above the superconducting transition temperature T_c and compacted again into two separated 'particles'. In this way the equi-chiral *wavy* entity is different to the photon, composed of two half-photons of opposed chirality and charge. The mathematical and experimental verification should be a worthwhile task for future cooperation. In this context the recent experimental observation of electron-exciton coupling in high-T_c cuprates is interesting [77].

In previous publications the present author connected the optimal concentration of superconducting carriers σ_0 with the fundamental number of the fifth power of the golden mean φ documenting the fractal nature of the electronic response in superconductors by the relation [16] [67] [78]

$$\sigma_0 \approx \frac{8}{\pi}\varphi^5 = 0.2296 \approx \frac{3}{13} \qquad (128)$$

However, we can also approximate σ_o by the mass constituents of the universe using relation (55) respectively (56), or following a relation using properties of the electron

$$\sigma_0 \approx \frac{\varphi^5}{\theta_{ea}} = 0.22928 \ldots \tag{129}$$

where $$\theta_{ea} = \int_{\beta_1}^{\beta_0} \frac{1}{\sqrt{1-\beta^2}} d\beta = \arcsin(\beta_0) - \arcsin(\beta_1) = 0.3932696 \ldots \tag{130}$$

using $\beta_0 = \frac{\sqrt{3}}{2}$ and $\beta_1 = 0.6083087$ [21]. In addition, we present the approximation

$$\theta_{ea} \approx \frac{\pi}{8} = 0.39269908 \tag{131}$$

Also the quotient of the *Fermi* speed v_F to the *Klitzing* speed v_K in superconductors gives a very simple approximation [67]

$$\frac{v_F}{v_K} \approx \frac{2}{\pi}\, \varphi^5 = 0.0571 \tag{132}$$

Furthermore, the superconducting transition temperature $T_{co}(K)$ is connected with the magic α constant (*Sommerfeld*'s constant) and the mean cationic charge $< q_c >$ by the quite simple relation

$$T_{co}(K) \propto 2740\ < q_c >^{-4} \approx \frac{20}{\alpha} < q_c >^{-4} \approx \frac{1}{|\beta_g|} < q_c >^{-4} \tag{133}$$

Surprisingly, the multiplier, which is involved in the hole pair creation, emerges as the fractal number δ_1, known as a universal scaling constant for two-dimensional maps in the theory of fractal systems or chaotic ones, with the precise value of δ_1 = 8.7210972…[79] [80]. Recently, *Savin et al*. [81] studied the self-oscillating system of the *Van der Pol* oscillator [82] subjected to an external force to compensate dissipation. Scaling constants δ_1 (and δ_2 = 2) have been determined as eigenvalues of the matrix containing the existence intervals of two subsequent cycles of the periodic-doubling cascade in the parameterized version of a quadratic *Hénon* map with renormalized (*x*,*y*)-parameters. We obtain for σ_0 [67]

$$\sigma_0 \approx \frac{2}{\delta_1} = 0.22933 \tag{134}$$

and $$\varphi^5 \approx \frac{\pi}{4 \cdot \delta_1} = 0.090057 \tag{135}$$

respectively $$\varphi^5 \approx \frac{2\theta_{ea}}{\delta_1} = 0.0901881 \tag{136}$$

However, the *Higgs* particle is by no means a God particle. We finish this chapter with a statement of the late *Nobel* laureate *Phil W. Anderson* 'Maybe the *Higgs* boson is fictitious' [83].

13. Approximating the In-Sphere Volume of a Soccer Ball

Interestingly, the in-sphere volume V_{sph} of a soccer ball having the structure of a truncated icosahedron with 32 faces and 60 vertices (60 C atoms) can be well approximated by the following relation showing a φ^{-5} term respectively a term including number 13 [27]

$$V_{sph} = \pi \cdot \frac{6^2}{5^3}\left(\frac{7\varphi^{-2}+\frac{\varphi}{6}}{2\sqrt{3}+(\varphi^3\sqrt{5})^{-\frac{1}{2}}}\right)^3 a^3 = \pi \cdot 15.89456977 \cdot a^3 \tag{138}$$

$$\approx \pi \cdot \left(\frac{4}{3}\right)^{\frac{5}{4}} \cdot \varphi^{-5}a^3 \approx \pi \cdot \sqrt[6]{\frac{13 \cdot 2}{3}} \cdot \varphi^{-5}a^3 = \pi \cdot 15.894500 \cdot \varphi^{-5}a^3$$

where *a* is the edge length of the pentagonal respectively hexagonal faces.

14. Honoring the Achievements of Past Civilizations

Dealing with the fifth power of the golden mean as omnipresent fundamental number it was still a surprise to find it in connection with the Great Pyramid at *Giza*. When calculating the ratio of the in-sphere volume V_O to the volume of the pyramid V_Δ respectively the corresponding surface ratio, we confirmed the following relation that connects the circle constant with the fifth power of the golden mean [27] [84] [85]

$$\frac{V_O}{V_\Delta} = \frac{S_O}{S_\Delta} = \pi \cdot \varphi^5 = 0.283277 \tag{137}$$

In this way, we obtain the exact fifth power of the golden mean simply by dividing the π-normalized in-sphere volume of the Great Pyramid by the volume of the Great Pyramid. This result is a tribute to the extraordinary skills of the ancient pyramid builders. Curious is the following solely π –based approximation (see relation 1e)

$$\frac{V_O}{V_\Delta} = \frac{S_O}{S_\Delta} \approx \frac{5\pi}{2}\left(\sqrt{\frac{6}{5\pi}} - \frac{6}{5\pi}\right) - \frac{\pi}{2} = 0.283268 \tag{138}$$

15. Unification Attempts

We can gain profit by creating more scientific clarity through physics unification attempts. The elaborated work of *Pellis* may be quoted here as pioneering [86]. The present author hopes that also his contribution is ground-breaking in one way or another. You don't need any great mathematical skill to understand the essentials.

16. Conclusion

This contribution shows the intimate connection between fundamental numbers, reciprocity relations and golden numbers, connecting the large and the small, and geometry in context to

life, physics and cosmos. The world is in steady rotational movement and is shaped by seemingly endless stochastic repetition actions. It explained the importance of quantities such as the circle constant π, *Sommerfeld*'s structure constant α, the golden mean φ and its fifth power φ^5 as well as the roll of structures such as helical twisting and the formation of icosahedral bodies. There are some evidence for our electron structure model proposed as icosahedral *Moebius* ball. Fundamental numbers may be considered as catalysts for life and cosmological processes. It cann't be ruled out that an icosahedral shaped vacuum condensate energy field provides the template for everything we observe. *Fibonacci* number 13 combined with its inverse are important in icosahedron mathematics as well as in life and may be important in computer sciences too. This number connects light and the electron and is hardly associated with misfortune or war, but is the number of wisdom and represents people's ability to think beyond the horizon. People who are trying to improve the world with artificial intelligence would be well advised to understand the heuristic concepts presented here. Once my late friend *Mohamed S. El Naschie* told me: 'I don't need a super-computer, because I work with the golden mean'.

Conflicts of Interest

The author declares no conflict of interests regarding the publication of this paper.

References

[1] Scheffen, M. et al. (2021) *Nature Catalysis* **4**, 105-115

[2] Deng, M., Yu, J. and Blackmond, D. G. (2024) Symmetry breaking and chiral amplification in prebiotic ligation reactions. *Nature* **626** (8001) 1019.

[3] Otto, H. H. (2024) Two Newly Introduced Angles Complete Our Geometrical Perception of Life, Physics and Cosmos. *ResearchGate*, 1-4.

[4] Otto, H. H. (2017) Should we pay more attention to the relationship between the golden mean and the Archimedes' constant? *Nonlinear Science Letters* A **8**, 410-412.

[5] Otto, H. H. (2024) Comment on *Trail*'s Fine Structure Constant Derivation. *ResearchGate*, 1-5.

[5a] Traill, D. (2019) Fine Structure Constant from the electron wave function. *ResearchGate*.

[6] Sigl, Ch., Willmer, E. M., Engelen, W., Kretzmann, J. A., Sachenbacher, K., Lidl, A. (2021) Programmable icosahedral shell structures. *Nature Materials* **20**,1281-1289.

[7] Otto, H. H. (2022) Golden Quartic Polynomial and Moebius-Ball Electron. *Journal of Applied Mathematics and Physics*, Volume **10,** 1785-1812.

[8] Sommerfeld, A. (1919) Atombau und Spektrallinien. Friedrich Vieweg & Sohn, Braunschweig.

[9] Klein, F. (1884) Vorlesungen über das Ikosaeder und die Auflösung der Gleichungen vom fünften Grad. Verlag B. G. Teubner, Leipzig

[10] Slodowy, P. (1986) Das Ikosaeder und die Gleichungen fünften Grades. *Arithmetik und Geometrie. Mathematische Miniaturen* **3**, 71-113 (Verlag Birkhäuser, Basel).

[11] Eschenburg, J. H. (1997) Das Ikosaeder und die Gleichungen 5. Grades nach Felix Klein. Seminar am Mathematischen Institut der Universität Augsburg, 8Nov. 1997 / Feb. !999), 1-29.

[12] Nash, O. (2013) On Klein's icosahedral solution of the quintic. *Expositiones Mathematicae* **32**, 99-120. DOI:10.1016/j.exmath.2013.09.003

[13] Gordon, P. (1869) Über die Auflösung der Gleichung vom fünften Grade. *Mathematische Annalen* **13**, 375-404.

[14] Pisano, L. (1202) Fibonacci's Liber Abaci (Book of Calculation). Biblioteca a Nazionale di Firenze.

[15] Otto, H. H. (2021) Beyond a Quartic Polynomial Modeling of the DNA Double-Helix Genetic Code. *Journal of Applied Mathematics and Physics* **9**, 2558-2577.
[16] Otto, H. H. (2020) Phase Transitions Governed by the Fifth Power of the Golden Mean and Beyond. *World Journal of Condensed Matter Physics* **10**, 135-159.
[17] Hardy, L. (1993) Nonlocality for Two Particles without Inequalities for Almost All Entangled States. *Physical Review Letters* **71**, 1665-1668.
[18] Mermin, N. D. (1994) Quantum mysteries refined. *American Journal of Physics* **62**, 880-887.
[19] Suleiman, R. (2019) Relativizing Newton. *Nova Science Publishers*, New York.
[20] Otto, H. H. (2017) Continued Fraction Representation of Universal Numbers and Approximations. *ResearchGate.net*. DOI:10.13140/RG.2.2.20110.66884, pp. 1-7.
[21] Guynn. P. (2018) Thomas precession is the basis for the structure of matter and space. *viXra*: 1810.0456, 1-27.
[22] Otto, H. H. (2022) Comment to Guynn's Fine-Structure Constant Approach. *Journal of Applied Mathematics and Physics* **10**, 2796-2804.
[23] The NIST Reference of Constants, Units and Uncertainty (2018), *NIST* Gaitherburg, MD 20899, USA.
[24] El Naschie, M. S. (2004) A Review of E-Infinity and the Mass Spectrum of High Energy Particle Physics. *Chaos, Solitons & Fractals* **19**, 209-236.
[25] Marec-Crnjak, L. (2013) Cantorian Space-Time Theory. *Lambert Academic Publishing*, Saarbrücken, 1-50.
[26] Olsen, S. (2006) The Golden Section: Nature's Greatest Secret. *Bloomsbury*, London, 64 p.
[27] Otto, H. H. (2021) Ratio of In-Sphere Volume to Polyhedron Volume of the Great Pyramid Compared to Selected Convex Polyhedral Solids. *Journal of Applied Mathematics and Physics* **9,** 41-56.
[28] Odom, B. (2004) Fully Quantum Measurement of the Electron Magnetic Momentum. *Thesis*, Harvard University, Massachusetts USA.
[29] Otto, H. H. (2018) Power Series Expansion Reveals the Fractal Properties of IRT Matter-Energy Transformation. *ResearchGate*, 1-4.
[30] Otto, H. H. (2025) Suleiman and Gyunn: Comparing Their Structure of Matter and Space Approaches. *viXra:2502.0157*, 1-4.
[31] Bennet, C. L. et al. (2013) Nine-Year Microwave Anisotropy Probe (WMAP) Observations: Final Maps and Results. *Astrophysical Journal Supplement Series* **208**, 20.
[32] Bouchet, F. R. (2016) Cosmology with the Planck Satellite: from quantum foam to the cosmic web. *Proceedings of Science* **268**, 1-22.
[33] Otto, H. H. (2024) Mass Constituents of the Universe: A Mathematical Chameleon Suggests New Physical Insights. *ResearchGate*
[34] El Naschie, M. S., Olsen, S., Helal, M. A., Marec-Crnjac and Nada, S. (2018) On the Missing Link between Cosmology and Biology. *International Journal of Innovation in Science and Mathematics* **6**, 11-13.
[35] El Naschie, M. S. (2004) A Review of E-Infinity and the Mass Spectrum of High Energy Particle Physics. *Chaos, Solitons & Fractals* **19**, 209-236.
[36] Cantor, G. (1932) Gesammelte Abhandlungen mathematischen und philosophischen Inhalts. *Springer*, Berlin.
[37] El Naschie, M. S. (2017) Elements of a New Set Theory Based Quantum Mechanics with Application in High Quantum Physics and Cosmology. *International Journal of High Energy Physics* **4**, 65-74.
[38] Urysohn, P. (1922) Les multiplicés Cantorennes. *Comptes Rendus* **175**, 440-442.
[39] Menger, K. (1928) Dimensionstheory. *Springer Verlag*, Leipzig und Berlin.
[40] Hausdorff, F. (1918) *Mathematische Annalen* **79**, 157-179.
[41] Otto, H. H. (2018) Mass Constituents of a Flat Lattice Multiverse: Conclusion From Similarity Between Two Universal Numbers, the Rocksalt-Type 2*D* Madelung Constant and the Golden Mean. *Journal of Modern Physics* **9**, 1-13.
[42] Otto, H. H. (2018) Reciprocity Relation between the Mass Constituents of the Universe and Hardy's Quantum Entanglement Probability. *World Journal of Condensed Matter Physics* **8**, 30-35.
[43] Otto, H. H. (2023) Creation of Paired Entities is Ever Governed by the Golden Mean: About the Nested Repeatability of Living and Cosmic Processes and the Origin of the Universe. *ResearchGate*, 1-14.
[44] Otto, H. H. (2023) Higgs Boson Mass Relations and Hole Superconductivity. *ResearchGate*, 1-14.

[45] ATLAS Experiments (2023): ATLAS sets record precision on Higgs boson mass. CERN Media Update, Juli 2023.
[46] Dirac, P. A. M. (1974) Cosmological Models and the Large Number Hypothesis. *Proceedings of the Royal Society of London* **A 338**, 439-446.
[47] Kosinov, M. (2023) Fractal Theory of Proton Mass: Fractal proton. The origin of constant m_p/m_e = 1836.1526… The law of baryogenesis. Fractal mechanism of baryonic asymmetry. *ResearchGate.net/publication* 374371975.
[48] Fang, F. Irwin, K., Kovacs, J. and Sadler, G. (2019) Cabinet of curiosities: the interesting geometry of the angle ß = arcos(3ϕ-1)/4). *Fractal and Fractional* **3**, 48.
[49] Pauling, L.C. (1945) The Nature of the Chemical Bond. Cornell Press Ithao, NY
[50] Moessner, R. and Ramirez, A. P. (2006) Geometric Frustration. *Physics Today* **59**, 24-29.
[51] Boltzmann, L. (1866) Über die Mechanische Bedeutung des Zweiten Hauptsatzes der Wärmetheorie. *Wiener Berichte* **53**, 195-220.
[52] Dragan, A. I., Crane-Robinson, C. and Privalov, P. L. (2021) Thermodynamic basis of the α-helix and DNA duplex. *European Biophysics Journal* **50**, 787-792.
[53] Casimir, H. B. G. (1948) On the attraction between two perfectly conducting plates. *Proceedings of the Koningklijke nederlandse Akademie van Wetenschappen* **B51**, 793-795.
[54] Bruisma, R. F., Gelbart, W. M., Reguera, D., Rudnick, J., and Zandi, R. (2003) Viral Self-Assembly as a Thermodynamic Process. *Physical Review Letters* **90**, 248101.1-4.
[55] Otto, H. H. und Ellner, M. (1987) Röntgenbeugungsuntersuchungen an quasikristallinem I-Al_4Mn. *Zeitschrift für Kristallographie* **178**, 178-179.
[56] Otto, H. H. (2024) Reciprocity Relation between Alternative Gravity Formulas. *Journal of Applied Mathematics and Physics* **12**, 1432-1440.
[57] Markoulakis, E. (2024) Superluminal Graviton Condensate Vacuum. *International Journal of Physical Research* **12**, 45-61.
[58] Weyl, H. (1929) Elektron und Graviton. I. *Zeitschrift für Physik* **56**, 330-352.
[59] Herring, C. (1937) Accidental Degeneracy in the Energy Bands of Crystals. *Physical Review* **52**, 365-373.
[60] Xu, S.-Y. et al. (2015) Discovery of a Weyl fermion semimetal and topological Fermi arcs. *Science* **349**, 613.
[61] Lee, C. (2015) Fermi surface interconnectivity and topology in Weyl fermion semimetals TaAs, TaP, NbAs, and NbP. *Physical Review* **B92**, 235104.
[62] Mikheenko, P. (2023) Superconductivity in self-assembled microtubules. *ResearchGate* 28649/1.
[63] Otto, H. H. (2024) Comment on Superconductivity in Self-Assembled Microtubules. *ResearchGate*.
[64] Otto, H. H. (2023) New Superionic Memory Devices Can Provide Clues to the Human Memory Structure and to Consciousness. *Journal of Applied Mathematics and Physics* **11,** 377-386.
[65] Otto, H. H. (2023) Could Pure Water Helices in a Supporting Helical Tube Scaffold Become Superconducting at Ambient Conditions of Temperature and Pressure? *ResearchGate*, 1-10.
[66] Ewald, P. (1921) Die Berechnung Optischer und Elektrostatischer Gitterpotentiale. *Annalen der Physik* **64**, 253-287.
[67] Otto, H. H. (2016) A Different Approach to High-T_c Superconductivity: Indication of Filamentary-Chaotic Conductance and Possible Routes to Superconductivity above Room Temperature. *World Journal of Condensed Matter Physics* **6**, 244-260.
[68] Littlewood, P. B. and Varma, C. M. (1982) Amplitude collective modes in superconductors and their coupling to charge-density waves. *Physical Review* **B26**, 4883-4893.
[69] Sherman, D. et al. (2015) The Higgs mode in distorted superconductors close to a quantum phase transition. *Nature Physics* **11**, 188-192.
[70] Schwarz, L. et al. (2020) Classification and Characterization of Nonequilibrium Higgs Modes in Unconventional Superconductors. *Nature Communications* **11**, Art.-No: 287.
[71] Nambu, Y. (1960) Quasiparticles and Gauge Invariance in the Theory of Superconductors. *Physical Review* **117**, 648-663.
[72] Goldstone, J. Salam, A., Weinberg, S. (1962) Broken Symmetries. *Physical Review* **127**, 965-970.
[73] Anderson, P. W. (1958) Coherent Excited States in the Theory of Superconductivity: Gauge Invariance and the Meissner Effect. *Physical Review* **110**, 827.

[74] Anderson, P. W. (2015) Higgs, Anderson and all that. *Nature Physics* **71**, 93.
[75] Le Phuong, H. et al (2020) High-precision measurement of Cooper pair mass using rotating spherical-shell superconductor. *Materials Letters* **262**, 127176.
[76] Hirsch, J. E. (2017) Why only hole conductors can be superconductors. *arXiv*:1703.09777v1 [cond-mat.supr-con].
[77] Barantani, F., Tran, M. K., Madan, I., Kapon, I., Bachar, N., Asmara, T. C., Paris, E., Tseng, Y., Zhang, W., Hu, Y., Giannini, E., Gu, G., Deveraux, T., P., Bertod, C., Carbone, E., Schmitt, T., and van der Marel, D. (2022) Experimental observation of electron-exciton coupling in high T_c cuprates. *ArXiv*:2108.06118v3 [cond-mat.supr-con], 1-10
[78] Otto, H. H. (2019) Super-Hydrides of Lanthanum and Yttrium: On Optimal Conditions for Achieving near Room Temperature Superconductivity. *World Journal of Condensed Matter Physics* **9**, 22-36.
[79] Hénon, M. (1976) A two-dimensional mapping with a strange attractor. *Communications in Mathematical Physics* **50**, 69-77.
[80] Hellmann, R.H.G. (1980) Self-generated chaotic behavior in nonlinear mechanics. *Fundamental problems in statistical mechanics* **5**, ed. E.G.D. Cohen, ed. North-Holland Publishing Company, Amsterdam.
[81] Savin, D.V., Savin, A.V., Kuznetsov, A.P., Kuznetsov, S.P. and Feudel, U. (2012) The self-oscillating system with compensated dissipation – the dymamics of the approcimate discrete map dynamical system.
[82] Van der Pol, B. (1922) On oscillation hysteresis in a triode generator with two degrees of freedom. *The London, Edinburgh, and Dublin Philosophical Magazine and Journal of Science Ser.* 6, **43**, 700-719.
[83] Anderson, P. W. (2015) Higgs, Anderson and all that. Nature Physics 11
[84] Otto, H. H. (2020) Magic Numbers of the Great Pyramid: A Surprising Result. *Journal of Applied Mathematics and Physics* **8,** 2063-2071**.**
[85] Otto, H. H. (2023) What Was the Real Reason for Building the Great Pyramid. *ResearchGate*, 1-15.
[86] Pellis, S. (2022) Dimensionless Unification of the Fundamental Interactions. *ResearchGate.net*, 1-19

Appendix

Table 4. Intrinsic Geometric Frustrations Suggested by the Split-Sphere-Volume Approach in Comparison with Other Fundamental Number Based Angular Relations

V_0/V_1	$\alpha_1(°)$	Condition
2.005309	50.911688	$\sqrt{2}\cdot 36° = \frac{1}{2}\arccos(\frac{\varphi}{2})$
2.000998	50.929581	$\frac{5\cdot 2^5}{\pi}$
2.000527	50.94871	$\varphi^2\cdot\frac{m_{Hi}}{m_p+m_e}$
2.000003	50.952703	$\varphi^2\cdot\sqrt{\alpha^{-1}\cdot N_{sd}}$
2.000000	50.952789	$V_0 = 2V_1$
1.999428	50.957217	$360\cdot\frac{16}{137.036-24}$
1.999209	50.958916	*Fibonacci* net
1.997683	50.970739	g_e based relation (10)
1.997345	50.973355	$\frac{\alpha_1}{360} = \pi - 3$
1.997333	50.973452	$360\cdot\frac{16}{137-24}$
1.996439	50.980384	7.140054944^2
1.995211	50.989902	$\frac{\alpha_1}{180} = \pi\cdot\varphi^5$

1.990487	51.026552	$h_1 = \varphi \cdot r_0$
1.986274	51.059277	$\pi^2 \cdot arcsin(\varphi^5)$

Roots of the Quartic Polynomial $\boldsymbol{P(x) = x^4 - 228x^3 + 494x^2 + 228x + 1}$

$$x_1 = -25 \cdot \sqrt{5} - 5 \cdot \sqrt{3} \cdot \sqrt{85 - 38 \cdot \sqrt{5}} + 57 = -0.387049270227545$$

$$x_2 = -25 \cdot \sqrt{5} + 5 \cdot \sqrt{3} \cdot \sqrt{85 - 38 \cdot \sqrt{5}} + 57 = 2.58365039523806$$

$$x_3 = +25 \cdot \sqrt{5} - 5 \cdot \sqrt{3} \cdot \sqrt{85 + 38 \cdot \sqrt{5}} + 57 = -0.00442854444608118$$

$$x_4 = +25 \cdot \sqrt{5} + 5 \cdot \sqrt{3} \cdot \sqrt{85 + 38 \cdot \sqrt{5}} + 57 = 225.807827419436$$

where $57 = \frac{228}{4}$, $38 = \frac{494}{13}$ and $5 \cdot \sqrt{5} = 11 + 2 \cdot \varphi^5$

Interestingly, $85 - 38 \cdot \sqrt{5} = 0.01315562 \cdot \sqrt{5}$

$$85 + 38 \cdot \sqrt{5} = 76.01315562 \cdot \sqrt{5}$$

where $0.01315562 = \frac{1}{76.01315562}$

belongs to the golden number series explained below using $N = 76^2 + 4 = 5780$.
We can verify also that the following relation well approximates number 13

$$\frac{\sqrt{3}}{2}\sqrt{x_1 + x_4} = 13.0025 \ldots \approx 13$$

Using the exact number, we can vice versa approximate the golden mean

$$\left(\frac{12}{13.0025}\right)^6 = 0.61791153$$

See also relation (24).

The Golden Numbers Series

$$N = \{4,5,8,13,20,29,40,53,68,85,104,125,148,173,200,229, \dots\}$$

The series shows differences of uneven numbers

$$N_{i+1} - N_i = \{1,3,5,7,9,11,13,15, \dots\}.$$

N can be obtained by square numbers N_i^2: $N = N_i^2 + 4$

Table 5. Golden Numbers Series (red) as Solution of a Depressed Quartic Polynomial

N	x_i	x_i^{-1}	$\sqrt{N} = x_i + x_i^{-1}$	$x_i - x_i^{-1}$
4.000	1.000000000000000	1.000000000000000	2.000000000000000	0.000000000000000
5.000	1.618033988749895	0.618033988749895	2.236067977499790	1.000000000000000
6.000	1.931851652578137	0.517638090205041	2.449489742783178	1.414213562373095
7.000	2.188901059316734	0.456850251747857	2.645751311064591	1.732050807568878
8.000	2.414213562373095	0.414213562373095	2.828427124746190	2.000000000000000
9.000	2.618033988749895	0.381966011250105	3.000000000000000	2.236067977499790
10.000	2.805883701475779	0.356393958692601	3.162277660168380	2.449489742783178
11.000	2.981188050709995	0.335436739645405	3.316624790355400	2.645751311064591
12.000	3.146264369941972	0.317837245195782	3.464101615137754	2.828427124746190
13.000	3.302775637731995	0.302775637731995	3.605551275463990	3.000000000000000
14.000	3.451967523471160	0.289689863302781	3.741657386773941	3.162277660168380
15.000	3.594804068281408	0.278179277926008	3.872983346207417	3.316624790355400
16.000	3.732050807568877	0.267949192431123	4.000000000000000	3.464101615137754
17.000	3.864328450540825	0.258777175076836	4.123105625617661	3.605551275463989
18.000	3.992149036946613	0.250491650172672	4.242640687119285	3.741657386773941
19.000	4.115941144874046	0.242957798666628	4.358898943540674	3.872983346207417
20.000	4.236067977499790	0.236067977499790	4.472135954999580	4.000000000000000
21.000	4.352840660286750	0.229735034669090	4.582575694955840	4.123105625617661
22.000	4.466528223471357	0.223887536352072	4.690415759823430	4.242640687119285
23.000	4.577365233426696	0.218466289886023	4.795831523312719	4.358898943540673
24.000	4.685557720282968	0.213421765283388	4.898979485566356	4.472135954999580
25.000	4.791287847477920	0.208712152522080	5.000000000000000	4.582575694955840
26.000	4.894717636708108	0.204301876884678	5.099019513592785	4.690415759823430
27.000	4.995991973009676	0.200160449696956	5.196152422706632	4.795831523312719
28.000	5.095241053847769	0.196261568281412	5.291502622129181	4.898979485566356
29.000	5.192582403567252	0.192582403567252	5.385164807134505	5.000000000000000
30.000	5.288122544322223	0.189103030729438	5.477225575051661	5.099019513592785
31.000	5.381958392768327	0.185805970061695	5.567764362830022	5.196152422706632
32.000	5.474178435810781	0.182675813681600	5.656854249492380	5.291502622129181
33.000	5.564863726836267	0.179698919701762	5.744562646538029	5.385164807134505
34.000	5.654088734948481	0.176863159896820	5.830951894845300	5.477225575051661
35.000	5.741922072964819	0.174157710134797	5.916079783099616	5.567764362830022
36.000	5.828427124746190	0.171572875253810	6.000000000000000	5.656854249492380

37.000	5.913662588418124	0.169099941880096	6.082762530298220	5.744562646538029
38.000	5.997682948907138	0.166731054061838	6.164414002968976	5.830951894845300
39.000	6.080538890749008	0.164459107649391	6.244997998398398	5.916079783099617
40.000	6.162277660168379	0.162277660168379	6.324555320336758	6.000000000000000
41.000	6.242943383865534	0.160180853567315	6.403124237432849	6.082762530298220
42.000	6.322577350688419	0.158163347719442	6.480740698407860	6.164414002968977
43.000	6.401218261350199	0.156220262951801	6.557438524302000	6.244997998398398
44.000	6.478902450523780	0.154347130187021	6.633249580710801	6.324555320336759
45.000	6.555664084966109	0.152539847533260	6.708203932499369	6.403124237432849
46.000	6.631535340766564	0.150794642358704	6.782329983125268	6.480740698407860
47.000	6.706546562351522	0.149108038049522	6.855654600401044	6.557438524302000
48.000	6.780726405493154	0.147476824782355	6.928203230275509	6.633249580710800
49.000	6.854101966249685	0.145898033750315	7.000000000000000	6.708203932499369
50.000	6.926698897495371	0.144368914370104	7.071067811865475	6.782329983125268
51.000	6.998541514471947	0.142886914070903	7.141428428542850	6.855654600401044
52.000	7.069652890601744	0.141449660326235	7.211102550927978	6.928203230275510
53.000	7.140054944640260	0.140054944640259	7.280109889280519	7.000000000000000
54.000	7.209768520107505	0.138700708242030	7.348469228349535	7.071067811865476
55.000	7.278813457819257	0.137385029276406	7.416198487095663	7.141428428542850
56.000	7.347208662237931	0.136106111309952	7.483314773547883	7.211102550927978
57.000	7.414972162275634	0.134862272995116	7.549834435270749	7.280109889280518
58.000	7.482121167106722	0.133651938757187	7.615773105863909	7.348469228349535
59.000	7.548672117482136	0.132473630386473	7.681145747868609	7.416198487095663
60.000	7.614640732981358	0.131325959433476	7.745966692414833	7.483314773547883
61.000	7.680042055588702	0.130207620317952	7.810249675906654	7.549834435270750
62.000	7.744890489937860	0.129117384073951	7.874007874011811	7.615773105863909
63.000	7.809199840531190	0.128054092662582	7.937253933193772	7.681145747868608
64.000	7.872983346207417	0.127016653792583	8.000000000000000	7.745966692414834
65.000	7.936253712102602	0.126004036195948	8.062257748298551	7.810249675906655
66.000	7.999023139323886	0.125015265312075	8.124038404635961	7.874007874011811
67.000	8.061303352533111	0.124049419339339	8.185352771872450	7.937253933193772
68.000	8.123105625617660	0.123105625617661	8.246211251235319	8.000000000000000
69.000	8.184440805608311	0.122183057309763	8.306623862918073	8.062257748298549
70.000	8.245319334988357	0.121280930352398	8.366600265340756	8.124038404635959
71.000	8.305751272524404	0.120398500651954	8.426149773176357	8.185352771872450
72.000	8.365746312736945	0.119535061501625	8.485281374238570	8.246211251235321
73.000	8.425313804117803	0.118689941199728	8.544003745317530	8.306623862918075
74.000	8.484462766191692	0.117862500850936	8.602325267042629	8.366600265340756
75.000	8.543201905510372	0.117052132334014	8.660254037844386	8.426149773176359
76.000	8.601539630659959	0.116258256421388	8.717797887081348	8.485281374238570
77.000	8.659484066354827	0.115480321037295	8.774964387392123	8.544003745317530
78.000	8.717043066685237	0.114717799642610	8.831760866327848	8.602325267042627
79.000	8.774224227579987	0.113970189735601	8.888194417315589	8.660254037844386
80.000	8.831034898540253	0.113237011458906	8.944271909999159	8.717797887081346
81.000	8.887482193696062	0.112517806303939	9.000000000000002	8.774964387392123
82.000	8.943573002232631	0.111812135904785	9.055385138137416	8.831760866327846
83.000	8.999313998229944	0.111119580914355	9.110433579144299	8.888194417315589
84.000	9.054711649955420	0.110439739956261	9.165151389911681	8.944271909999159
85.000	9.109772228646444	0.109772228646444	9.219544457292887	9.000000000000000
86.000	9.164501816816561	0.109116678679144	9.273618495495704	9.055385138137417

87.000	9.218906316116557	0.108472736972258	9.327379053088816	9.110433579144299
88.000	9.272991454779270	0.107840064867590	9.380831519646860	9.165151389911680
89.000	9.326762794674746	0.107218337381858	9.433981132056605	9.219544457292887
90.000	9.380225738000421	0.106607242504717	9.486832980505138	9.273618495495704
91.000	9.433385533629135	0.106006480540321	9.539392014169456	9.327379053088814
92.000	9.486247283136148	0.105415763489290	9.591663046625438	9.380831519646858
93.000	9.538815946524780	0.104834814468176	9.643650760992955	9.433981132056605
94.000	9.591096347668898	0.104263367163760	9.695359714832659	9.486832980505138
95.000	9.643093179489211	0.103701165319754	9.746794344808965	9.539392014169458
96.000	9.694811008879077	0.103147962253637	9.797958971132713	9.591663046625440
97.000	9.746254281394529	0.102603520401575	9.848857801796104	9.643650760992955
98.000	9.797427325722161	0.102067610889504	9.899494936611665	9.695359714832657
99.000	9.848334357937581	0.101540013128618	9.949874371066199	9.746794344808963
100.00	9.898979485566356	0.101020514433644	10.000000000000000	9.797958971132712
101.00	9.949366711458497	0.100508909662393	10.049875621120890	9.848857801796104
102.00	9.999499937486872	0.100005000875206	10.099504938362079	9.899494936611665
103.00	10.049382968079209	0.099508597013010	10.148891565092219	9.949874371066199
104.00	10.099019513592784	0.099019513592785	10.198039027185569	10.000000000000000
105.00	10.148413193540245	0.098537572419354	10.246950765959600	10.049875621120890
106.00	10.197567539674539	0.098062601312461	10.295630140987001	10.099504938362077
107.00	10.246485998940411	0.097594433848190	10.344080432788601	10.148891565092221
108.00	10.295171936299417	0.097132909113847	10.392304845413264	10.198039027185569
109.00	10.343628637435074	0.096677871475476	10.440306508910551	10.246950765959598
110.00	10.391859311344257	0.096229170357258	10.488088481701515	10.295630140986999
111.00	10.439867092820670	0.095786660032069	10.535653752852738	10.344080432788601
112.00	10.487655044835813	0.095350199422549	10.583005244258363	10.392304845413264
113.00	10.535226160822599	0.094919651912050	10.630145812734648	10.440306508910551
114.00	10.582583366866412	0.094494885164898	10.677078252031309	10.488088481701515
115.00	10.629729523808173	0.094075770955435	10.723805294763608	10.535653752852738
116.00	10.676667429263684	0.093662185005323	10.770329614269007	10.583005244258361
117.00	10.723399819563308	0.093254006828659	10.816653826391967	10.630145812734650
118.00	10.769929371615763	0.092851119584452	10.862780491200215	10.677078252031311
119.00	10.816258704699662	0.092453409936053	10.908712114635716	10.723805294763608
120.00	10.862390382186165	0.092060767917157	10.954451150103322	10.770329614269007
121.00	10.908326913195983	0.091673086804016	11.000000000000000	10.816653826391967
122.00	10.954070754193738	0.091290262993523	11.045361017187261	10.862780491200215
123.00	10.999624310522567	0.090912195886851	11.090536506409418	10.908712114635716
124.00	11.044989937881683	0.090538787778361	11.135528725660043	10.954451150103322
125.00	11.090169943749475	0.090169943749474	11.180339887498949	11.000000000000000
126.00	11.135166588754542	0.089805571567282	11.224972160321824	11.045361017187259
127.00	11.179982087997031	0.089445581587614	11.269427669584644	11.090536506409418
128.00	11.224618612322402	0.089089886662358	11.313708498984761	11.135528725660043
129.00	11.269078289549748	0.088738402050799	11.357816691600547	11.180339887498949
130.00	11.313363205656602	0.088391045334778	11.401754250991379	11.224972160321824
131.00	11.357475405922122	0.088047736337476	11.445523142259598	11.269427669584646
132.00	11.401416896030408	0.087708397045648	11.489125293076057	11.313708498984759
133.00	11.445189643135672	0.087372951535124	11.532562594670797	11.357816691600547
134.00	11.488795576890803	0.087041325899423	11.575836902790225	11.401754250991381
135.00	11.532236590440924	0.086713448181327	11.618950038622250	11.445523142259598
136.00	11.575514541383329	0.086389248307272	11.661903789690601	11.489125293076057

137.00	11.618631252695209	0.086068658024415	11.704699910719624	11.532562594670795
138.00	11.661588513630479	0.085751610840253	11.747340124470732	11.575836902790225
139.00	11.704388080586924	0.085438041964673	11.789826122551597	11.618950038622250
140.00	11.747031677944916	0.085127888254316	11.832159566199232	11.661903789690600
141.00	11.789520998878771	0.084821088159146	11.874342087037917	11.704699910719626
142.00	11.831857706141857	0.084517581671127	11.916375287812984	11.747340124470730
143.00	11.874043432826497	0.084217310274901	11.958260743101398	11.789826122551595
144.00	11.916079783099617	0.083920216900384	12.000000000000002	11.832159566199232
145.00	11.957968332915106	0.083626245877189	12.041594578792296	11.874342087037917
146.00	11.999710630703779	0.083335342890794	12.083045973594572	11.916375287812986
147.00	12.041308198041769	0.083047454940372	12.124355652982141	11.958260743101397
148.00	12.082762530298220	0.082762530298220	12.165525060596440	12.000000000000000
149.00	12.124075097262999	0.082480518470704	12.206555615733702	12.041594578792296
150.00	12.165247343755231	0.082201370160659	12.247448713915890	12.083045973594572
151.00	12.206280690213324	0.081925037231183	12.288205727444508	12.124355652982141
152.00	12.247176533267197	0.081651472670757	12.328828005937954	12.165525060596440
153.00	12.287936246293343	0.081380630559639	12.369316876852983	12.206555615733704
154.00	12.328561179953374	0.081112466037483	12.409673645990857	12.247448713915890
155.00	12.369052662716619	0.080846935272112	12.449899597988733	12.288205727444506
156.00	12.409412001367375	0.080583995429422	12.489995996796797	12.328828005937954
157.00	12.449640481497324	0.080323604644343	12.529964086141668	12.369316876852981
158.00	12.489739367983695	0.080065721992839	12.569805089976533	12.409673645990857
159.00	12.529709905453611	0.079810307464880	12.609520212918492	12.449899597988731
160.00	12.569553318735156	0.079557321938360	12.649110640673516	12.489995996796797
161.00	12.609270813295595	0.079306727153926	12.688577540449522	12.529964086141668
162.00	12.648863575667194	0.079058485690660	12.727922061357855	12.569805089976533
163.00	12.688332773861099	0.078812560942607	12.767145334803706	12.609520212918492
164.00	12.727679557769607	0.078568917096090	12.806248474865697	12.649110640673516
165.00	12.766905059557324	0.078327519107804	12.845232578665128	12.688577540449520
166.00	12.806010394041490	0.078088332683635	12.884098726725124	12.727922061357855
167.00	12.844996659061895	0.077851324258190	12.922847983320086	12.767145334803704
168.00	12.883864935840709	0.077616460975012	12.961481396815721	12.806248474865697
169.00	12.922616289332565	0.077383710667436	13.000000000000000	12.845232578665129
170.00	12.961251768565212	0.077153041840086	13.038404810405298	12.884098726725126
171.00	12.999772406971053	0.076924423650968	13.076696830622019	12.922847983320086
172.00	13.038179222709861	0.076697825894140	13.114877048604001	12.961481396815721
173.00	13.076473218982953	0.076473218982953	13.152946437965905	13.000000000000000
174.00	13.114655384339109	0.076250573933811	13.190905958272920	13.038404810405298
175.00	13.152726692972486	0.076029862350466	13.228756555322953	13.076696830622019
176.00	13.190688105012800	0.075811056408799	13.266499161421599	13.114877048604001
177.00	13.228540566807988	0.075594128842083	13.304134695650070	13.152946437965905
178.00	13.266285011199626	0.075379052926707	13.341664064126332	13.190905958272920
179.00	13.303922357791302	0.075165802468350	13.379088160259652	13.228756555322953
180.00	13.341453513210169	0.074954351788569	13.416407864998739	13.266499161421599
181.00	13.378879371361890	0.074744675711820	13.453624047073710	13.304134695650070
182.00	13.416200813679188	0.074536749552854	13.490737563232042	13.341664064126334
183.00	13.453418709364167	0.074330549104515	13.527749258468683	13.379088160259650
184.00	13.490533915624637	0.074126050625899	13.564659966250536	13.416407864998737
185.00	13.527547277904576	0.073923230830867	13.601470508735442	13.453624047073710
186.00	13.564459630108949	0.073722066876907	13.638181696985857	13.490737563232042

187.00	13.601271794823013	0.073522536354330	13.674794331177344	13.527749258468683
188.00	13.637984583526311	0.073324617275776	13.711309200802088	13.564659966250534
189.00	13.674598796801481	0.073128288066038	13.747727084867520	13.601470508735442
190.00	13.711115224538039	0.072933527552183	13.784048752090222	13.638181696985857
191.00	13.747534646131298	0.072740314953955	13.820274961085254	13.674794331177342
192.00	13.783857830676553	0.072548629874465	13.856406460551018	13.711309200802088
193.00	13.820085537158663	0.072358452291142	13.892443989449806	13.747727084867520
194.00	13.856218514637170	0.072169762546949	13.928388277184119	13.784048752090222
195.00	13.892257502427096	0.071982541341844	13.964240043768941	13.820274961085252
196.00	13.928203230275509	0.071796769724491	14.000000000000000	13.856406460551018
197.00	13.964056418534001	0.071612429084198	14.035668847618199	13.892443989449804
198.00	13.999817778327204	0.071429501143085	14.071247279470288	13.928388277184119
199.00	14.035488011717414	0.071247967948472	14.106735979665885	13.964240043768942
200.00	14.071067811865476	0.071067811865475	14.142135623730951	14.000000000000000
201.00	14.106557863188012	0.070889015569813	14.177446878757825	14.035668847618199
202.00	14.141958841511091	0.070711562040803	14.212670403551893	14.071247279470288
203.00	14.177271414220446	0.070535434554561	14.247806848775006	14.106735979665885
204.00	14.212496240408324	0.070360616677375	14.282856857085699	14.142135623730949
205.00	14.247633971017089	0.070187092259264	14.317821063276353	14.177446878757825
206.00	14.282685248979609	0.070014845427714	14.352700094407323	14.212670403551895
207.00	14.317650709356583	0.069843860581576	14.387494569938159	14.247806848775006
208.00	14.352530979470828	0.069674122385129	14.422205101855956	14.282856857085699
209.00	14.387326679038658	0.069505615762304	14.456832294800961	14.317821063276355
210.00	14.422038420298382	0.069338325891057	14.491376746189440	14.352700094407323
211.00	14.456666808136054	0.069172238197896	14.525839046333950	14.387494569938159
212.00	14.491212440208496	0.069007338352540	14.560219778561036	14.422205101855956
213.00	14.525675907063691	0.068843612262732	14.594519519326424	14.456832294800959
214.00	14.560057792258617	0.068681046069177	14.628738838327793	14.491376746189440
215.00	14.594358672474565	0.068519626140615	14.662878298615180	14.525839046333950
216.00	14.628579117630052	0.068359339069016	14.696938456699067	14.560219778561036
217.00	14.662719690991329	0.068200171664906	14.730919862656235	14.594519519326424
218.00	14.696780949280598	0.068042110952804	14.764823060233400	14.628738838327795
219.00	14.730763442781962	0.067885144166781	14.798648586948742	14.662878298615182
220.00	14.764667715445198	0.067729258746129	14.832396974191326	14.696938456699069
221.00	14.798494304987370	0.067574442331135	14.866068747318506	14.730919862656235
222.00	14.832243742992370	0.067420682758970	14.899664425751340	14.764823060233400
223.00	14.865916555008411	0.067267968059668	14.933184523068080	14.798648586948742
224.00	14.899513260643545	0.067116286452220	14.966629547095765	14.832396974191324
225.00	14.933034373659252	0.066965626340747	15.000000000000000	14.866068747318504
226.00	14.966480402062123	0.066815976310784	15.033296378372906	14.899664425751340
227.00	14.999851848193721	0.066667325125642	15.066519173319364	14.933184523068078
228.00	15.033149208818633	0.066519661722867	15.099668870541500	14.966629547095767
229.00	15.066372975210779	0.066372975210778	15.132745950421556	15.000000000000000
230.00	15.099523633238004	0.066227254865096	15.165750888103100	15.033296378372908
231.00	15.132601663445014	0.066082490125650	15.198684153570664	15.066519173319364
232.00	15.165607541134658	0.065938670593159	15.231546211727817	15.099668870541500
233.00	15.198541736447652	0.065795786026096	15.264337522473747	15.132745950421556
234.00	15.231404714440728	0.065653826337627	15.297058540778355	15.165750888103101
235.00	15.264196935163277	0.065512781592614	15.329709716755891	15.198684153570662
236.00	15.296918853732517	0.065372642004700	15.362291495737217	15.231546211727817

237.00	15.329570920407200	0.065233397933452	15.394804318340652	15.264337522473747
238.00	15.362153580659934	0.065095039881579	15.427248620541512	15.297058540778355
239.00	15.394667275248100	0.064957558492207	15.459624833740307	15.329709716755893
240.00	15.427112440283443	0.064820944546226	15.491933384829668	15.362291495737217
241.00	15.459489507300338	0.064685188959686	15.524174696260024	15.394804318340652
242.00	15.491798903322779	0.064550282781266	15.556349186104045	15.427248620541514
243.00	15.524041050930101	0.064416217189795	15.588457268119896	15.459624833740307
244.00	15.556216368321488	0.064282983491821	15.620499351813308	15.491933384829668
245.00	15.588325269379276	0.064150573119252	15.652475842498527	15.524174696260024
246.00	15.620368163731083	0.064018977627038	15.684387141358121	15.556349186104045
247.00	15.652345456810803	0.063888188690908	15.716233645501710	15.588457268119896
248.00	15.684257549918465	0.063758198105157	15.748015748023622	15.620499351813308
249.00	15.716104840279014	0.063628997780486	15.779733838059499	15.652475842498529
250.00	15.747887721100009	0.063500579741887	15.811388300841896	15.684387141358121
251.00	15.779606581628286	0.063372936126574	15.842979517754861	15.716233645501712
252.00	15.811261807205582	0.063246059181961	15.874507866387543	15.748015748023622